IEEE Photonics Journal
An IEEE Photonics Society Publication

Open Access

Single-Shot Imaging Without Reference Wave Using Binary Intensity Pattern for Optically-Secured-Based Correlation

Volume 8, Number 1, February 2016

Wen Chen

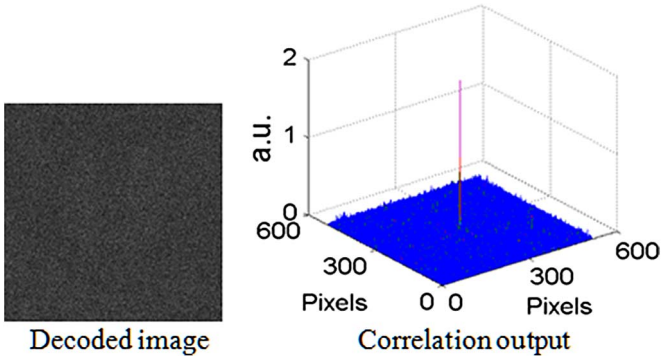

DOI: 10.1109/JPHOT.2016.2523245
1943-0655 © 2016 IEEE

IEEE photonics SOCIETY

IEEE

Single-Shot Imaging Without Reference Wave Using Binary Intensity Pattern for Optically-Secured-Based Correlation

Wen Chen

Department of Electronic and Information Engineering, The Hong Kong Polytechnic University, Kowloon, Hong Kong, China

DOI: 10.1109/JPHOT.2016.2523245

Manuscript received December 15, 2015; revised January 23, 2016; accepted January 26, 2016. Date of publication January 28, 2016; date of current version February 9, 2016. This work was supported by the startup grant (1-ZE5F) from The Hong Kong Polytechnic University. Corresponding author: W. Chen (e-mail: owen.chen@polyu.edu.hk).

Abstract: In this paper, a novel method is proposed to optically verify the decoded images via single-shot imaging without reference wave using a binary intensity pattern. Optical imaging without reference wave is applied based on double random phase encoding (DRPE), and the recorded intensity pattern is further compressed, which contains only two quantization levels (i.e., 0 and 1). During the decoding, an iterative phase retrieval algorithm is developed and applied. It is demonstrated that decoded images do not visually render the input information due to the designed optical encoding strategy using only one binary intensity pattern, and optical verification is further conducted to effectively verify the decoded images. An additional security layer is established for the developed optical system, since optical verification is conducted based on optical encoding systems without direct observation of input information from the decoded images. It is the first to report the use of only one 1-bit intensity pattern in the DRPE system based on single-shot imaging without reference wave for secured verification via optical correlation.

Index Terms: Single-pixel imaging, computational imaging, binary intensity pattern, optical correlation.

1. Introduction

Since double random phase encoding (DRPE) [1] was proposed by Refregier and Javidi, optical encoding [2]–[5] has attracted much attention due to its marked advantages, such as parallel processing and multiple dimensions. In DRPE system, the input image can be converted into stationary white noise by using two statistically independent random phase-only masks, respectively, placed in the input plane and spatial frequency plane [1]–[5]. Random phase-only mask in the input plane makes the signal white but nonstationary, and random phase-only mask in the spatial frequency plane maintains the whiteness but makes it stationary with signal encryption [1]–[3], [5]. Various infrastructures and algorithms [6]–[19], such as nonlinear [13], [14], have been developed to enrich optical encoding field. It has also been demonstrated that the input data can be encoded in various transform domains, such as Fresnel [6], [7] and fractional Fourier [8].

It has been found that DRPE system may be attacked [20] due to its linear characteristic. Some approaches have been developed to mitigate the possible weakness of conventional DRPE system. Scrambling algorithms [21], [22] are applied to the optical security system for the

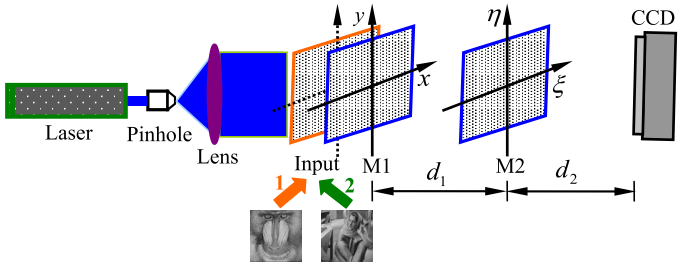

Fig. 1. Schematic setup for the proposed method. M1 and M2: random phase-only masks; CCD: charge-coupled device. The second input image (8 bits and 512 × 512 pixels) is used for testing discrimination capability, and phase-only mask M1 is placed just behind the input image. The input images are from http://sipi.usc.edu/database.

enhancement of system security; however, the additional algorithms might prevent convenient implementations of fully optical encoding. Frauel *et al.*, [23] have proposed several methods for DRPE system against the attacks, and it has been illustrated that updating keys is one effective approach to enhance system security. Kumar *et al.*, [24] applied the randomized lens-phase functions against impulse attack. Recently, optical information authentication based on DRPE using photon counting [25] has been developed to enhance system security. However, wavefront larger than 1 bit in the detector plane is still requested, and the sparse phase in the detector plane should be extracted for the decoding. In addition, relatively complex setup, such as polarization or interference, is usually applied to extract sparse wavefront (including amplitude and phase) in the detector plane.

In this paper, a novel method is proposed for optically verifying the decoded images based on single-shot imaging using binary intensity pattern. During optical encoding, imaging without reference wave is applied based on DRPE infrastructure and the recorded intensity pattern is further compressed which contains only two quantization levels, i.e., 0 and 1. During the decoding, iterative phase retrieval algorithm is developed and applied to extract the decoded images. It will be illustrated that the decoded images do not visually render the input information due to the designed optical encoding strategy using a binary intensity pattern, and nonlinear correlation algorithm [25]–[27] can be applied as an effective approach to optically verify the decoded images.

2. Theoretical Analysis

Fig. 1 shows a schematic setup for the proposed optical system. Random phase-only masks M1 and M2 are placed, respectively, in the input plane and Fresnel domain, however it can be straightforward to apply other transform domains [8], [18] in the proposed optical system. Here, $M_1(x, y)$ and $M_2(\xi, \eta)$, respectively, denote phase-only masks M1 and M2, randomly distributed in a range of $[0, 2\pi]$. In the proposed optical system, the encoding process is described by

$$I_o(\mu, \nu) = \left|\mathrm{FrT}_{\lambda, d_2}\left(\left\{\mathrm{FrT}_{\lambda, d_1}[O(x, y)M_1(x, y)]\right\}M_2(\xi, \eta)\right)\right|^2 \tag{1}$$

$$I(\mu, \nu) = \begin{cases} 1 & I_o(\mu, \nu) \geq \text{threshold} \\ 0 & I_o(\mu, \nu) < \text{threshold} \end{cases} \tag{2}$$

where (x, y), (ξ, η) and (μ, ν), respectively, denote coordinates of the input plane, phase-only mask (M2) plane and CCD plane, $O(x, y)$ denotes an input image (8 bits and 512 × 512 pixels), $I(\mu, \nu)$ denotes the encoded image (i.e., ciphertexts) after data compression, λ denotes the laser wavelength, d_1 and d_2 denote axial distances, $|\ |$ denotes modulus operation, and FrT denotes free-space wave propagation [28]. Since the compression method is applied, only two quantization levels, i.e., 0 and 1, are available. The threshold can be flexibly adjusted [29], and histogram equalization [30] is one effective and applicable approach. In conventional optical methods, interference principle, such as off-axis and in-line holography [1]–[3], [5]–[7], [25], is usually employed for optical encoding. In this study, single-shot coherent imaging is applied

without reference wave, and there are several remarkable characteristics, such as simple setup and robustness to external vibrations.

For the decoding, an iterative phase retrieval algorithm based on modified Gerchberg-Saxton algorithm [31] is developed and applied. Let $O^{(n)}(x,y)$ denote the estimated input image at the nth iteration $(n=1,2,3,\ldots,N)$, and the initially estimated plaintext is randomly distributed in a range of $[0,2\pi]$. In the proposed optical system, only one binary diffraction intensity pattern, i.e., ciphertext, is available, and the decoding process consists of following steps:

1) Propagate forward to the CCD plane:

$$O^{(n)}(\mu,\nu)=\mathrm{FrT}_{\lambda,d_2}\left(\left\{\mathrm{FrT}_{\lambda,d_1}\left[O^{(n)}(x,y)M_1(x,y)\right]\right\}M_2(\xi,\eta)\right). \tag{3}$$

2) A constraint with binary diffraction intensity pattern $I(\mu,\nu)$ is applied to update amplitude part of complex amplitude $O^{(n)}(\mu,\nu)$:

$$\hat{O}^{(n)}(\mu,\nu)=I(\mu,\nu)\left[\frac{O^{(n)}(\mu,\nu)}{|O^{(n)}(\mu,\nu)|}\right]. \tag{4}$$

3) Propagate back to the input plane:

$$\hat{O}^{(n)}(x,y)=\left[\mathrm{FrT}_{\lambda,-d_1}\left(\left\{\mathrm{FrT}_{\lambda,-d_2}\left[\hat{O}^{(n)}(\mu,\nu)\right]\right\}[M_2(\xi,\eta)]^*\right)\right][M_1(x,y)]^* \tag{5}$$

where $\mathrm{FrT}_{\lambda,-d_1}$ and $\mathrm{FrT}_{\lambda,-d_2}$ denote wave back-propagation [28], asterisk denotes complex conjugate, and $\hat{O}^{(n)}(x,y)$ denotes the updated wavefront related to the input image. After Eqs. (3)–(5) are implemented, iterative error is defined and calculated to judge whether the iterative process can be stopped.

$$\mathrm{Error}=\sum_{x,y}\left[\left|\hat{O}^{(n)}(x,y)\right|-\left|\hat{O}^{(n-1)}(x,y)\right|\right]^2. \tag{6}$$

If the calculated iterative error is still larger than a preset threshold (ε), amplitude part of the updated complex amplitude $\hat{O}^{(n)}(x,y)$ [see (5)] is used as a new estimate for the next iteration $(n=n+1)$, i.e., replacing $O^{(n)}(x,y)$ in (3) with $|\hat{O}^{(n)}(x,y)|$. The aforementioned iterative process is implemented until the preset threshold is satisfied. Once the iterative process is completed, amplitude part of the finally updated wavefront [i.e., $|\hat{O}^{(N)}(x,y)|$] is considered as a decoded image $O'(x,y)$. An evaluation function [3], [12] is applied to evaluate quality of the decoded image, and correlation coefficient (CC) is applied here and calculated by

$$\mathrm{CC}=\frac{[\mathrm{cov}(O,O')]}{(\sigma_O\times\sigma_{O'})} \tag{7}$$

where cov denotes cross-covariance, and σ denotes standard deviation. For brevity, the coordinate (x,y) is omitted in (7).

Since only one binary diffraction intensity pattern is available for the decoding, the decoded images do not visually render the input information. Even when a low-pass filter [32] is applied to process the amplitude part of complex-valued wavefront $\hat{O}^{(n)}(x,y)$ [see Eq. (5)] during the iterations, no information related to input image can be directly observed from the decoded images (see results in Section 3). Here, optical verification based on nonlinear correlation algorithm [4], [25]–[27], [33] is applied to authenticate the decoded images, and the verification function is described by

$$NC(x,y)=\left|\mathrm{IFT}\left(\left|\{\mathrm{FT}[O(x,y)]\}\{\mathrm{FT}[O'(x,y)]\}^*\right|^{p-1}\{\mathrm{FT}[O(x,y)]\}\{\mathrm{FT}[O'(x,y)]\}^*\right)\right|^2 \tag{8}$$

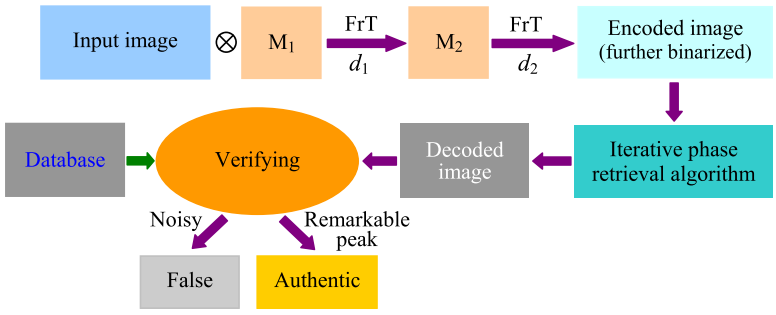

Fig. 2. Flow chart for schematically illustrating optical encoding, decoding, and verification processes based on the proposed optical system. ⊗ denotes a multiplication operation.

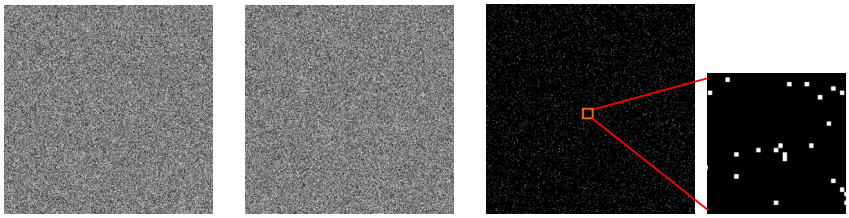

Fig. 3. (a) Phase-only mask M1, (b) Phase-only mask M2, and (c) the encoded image. The small area in (c) is enlarged to clearly illustrate that only binary data are available and the encoded image is highly compressed (white pixels are equivalent to one, and others are zero).

where $NC(x, y)$ denotes the generated nonlinear correlation map; FT and IFT, respectively, denote Fourier transform and inverse Fourier transform [25]–[27], and p denotes the strength of applied nonlinearity [25]–[27]. Here, the parameter p is set as 0.30. It should be emphasized that different from conventional optical encoding methods [1]–[3], [5]–[10], major objective of the proposed optical system is to conduct information verification based on optical encoding system rather than to clearly observe the input image during optical decoding. In practice, the original input image can be stored in the separated or remote database [34], and only one interface is given for the receiver to conduct the verification without direct disclosure of original input image [34]. A flow chart is shown in Fig. 2 to clearly illustrate the optical encoding, decoding, and verification processes described previously.

3. Results and Discussion

The schematic setup shown in Fig. 1 is numerically conducted to show feasibility and effectiveness of the proposed method. The collimated plane wave is generated by combination of a pinhole and lens, and light wavelength is 630.0 nm. The phase-only masks M1 and M2 as shown in Fig. 3(a) and (b) are randomly distributed in a range of $[0, 2\pi]$, respectively placed in the input plane and Fresnel domain. Application of other transform domains [8], [18] can be straightforward for the proposed optical system. Axial distances d_1 and d_2 are 15.0 cm and 25.0 cm, respectively. During optical encoding, only one binary diffraction intensity pattern, i.e., each pixel containing either 0 or 1, is further generated as the ciphertext. In practice, the threshold can be flexibly designed and adjusted [29], [30], and Fig. 3(c) shows the encoded image, i.e., binary intensity pattern. Here, the threshold is equivalent to 3.7 times the average value of intensity pattern $I_o(\mu, \nu)$ [see (1)]. A small area has been enlarged as shown in Fig. 3(c) to clearly illustrate that only binary data are obtained. It is also illustrated in Fig. 3(c) that the diffraction intensity pattern $I(\mu, \nu)$ is highly compressed.

Fig. 4(a) shows a relationship between the number of iterations and iterative errors (logarithm scale) during the decoding, when all keys are correctly applied. Here, the threshold (ε) used for

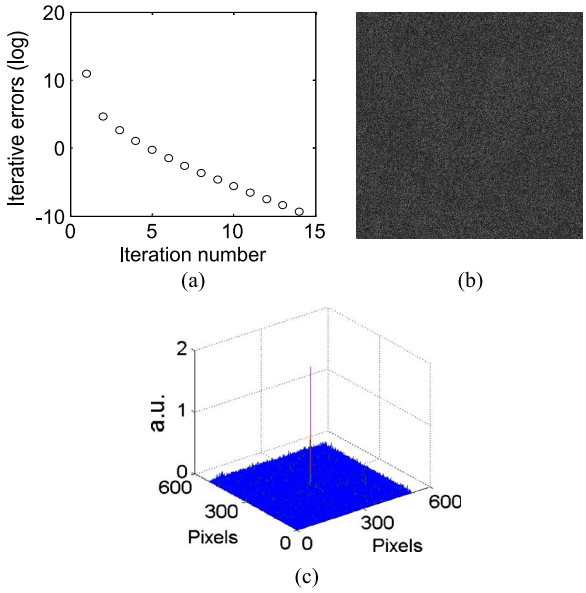

Fig. 4. (a) Relationship between the number of iterations and iterative errors (logarithm scale) during the decoding when all keys are correctly applied, (b) the decoded image, and (c) the generated nonlinear correlation distribution corresponding to (b).

iterative phase retrieval algorithm is preset as 1.0×10^{-4}. It can be seen in Fig. 4(a) that a rapid convergence rate, i.e., only 14 iterations, is achieved. Fig. 4(b) shows the correspondingly decoded image. The CC value for Fig. 4(b) is 5.75×10^{-2}. It is seen in Fig. 4(b) that no information related to input image can be observed from the decoded image due to the designed optical encoding strategy using only one binary intensity pattern. This decoded image can be further verified by using nonlinear correlation algorithm, since it still contains some useful but invisible data related to original input image. Fig. 4(c) shows the generated nonlinear correlation distribution corresponding to Fig. 4(b). Only one remarkable peak is obtained in the generated nonlinear correlation map, which means the decoded image being authentic. For the receivers, the decoding operation should be first implemented, and the decoded image can be compared and correlated with the original input image stored in the remote or separated database. It should be emphasized that in this case, only one interface should be designed to allow the verification operation for the receiver who also cannot directly see the original input image [34]. Due to this design, an additional security layer has been established for DRPE system.

Since information verification is developed based on optical encoding, system parameters, such as phase-only masks, distances, and wavelength, play an important role as those in conventional optical encoding systems [1]–[3], [5]–[8]. Performance of these parameters is further analyzed here. Fig. 5(a) and (b) show the decoded images, when only phase-only mask M1 or M2 is wrongly used during the decoding, respectively. The CC values for Fig. 5(a) and (b) are -9.8×10^{-4} and -1.4×10^{-3}, respectively. Fig. 6(a) and (b) show the generated nonlinear correlation distributions corresponding to Fig. 5(a) and (b), respectively. Noisy background is observed, which means that the receiver does not possess correct keys and he or she is not the authorized receiver. Similarly, when only axial distance (i.e., distance d_1 with an error of 1.0 cm) or wavelength (i.e., an error of 10.0 nm) is incorrectly applied during the decoding, noisy correlation distributions are also obtained as shown in Fig. 6(c) and (d) respectively corresponding to the decoded images in Fig. 5(c) and (d). The CC values for Fig. 5(c) and (d) are -3.1×10^{-4} and 5.9×10^{-4}, respectively. It is worth noting that major objective of the proposed optical system is to conduct optical verification based on optical encoding system rather than to clearly observe the input image from the decoded images usually pursued in conventional optical encoding systems [3].

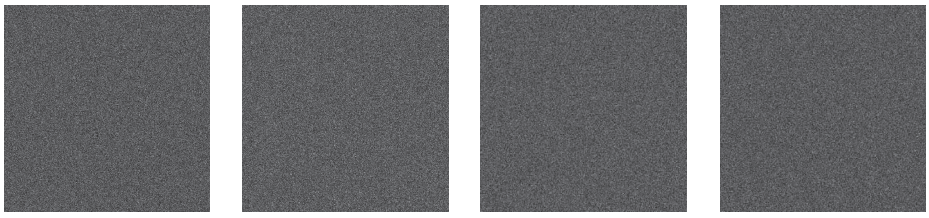

Fig. 5. Decoded images obtained when (a) only phase-only mask M1 or (b) only M2 is wrongly used during the decoding, (c) decoded image obtained when only axial distance d_1 contains an error of 1.0 cm during the decoding, and (d) decoded image obtained when only light wavelength contains an error of 10.0 nm during the decoding. The 500 iterations are applied for each decoding in (a)–(d).

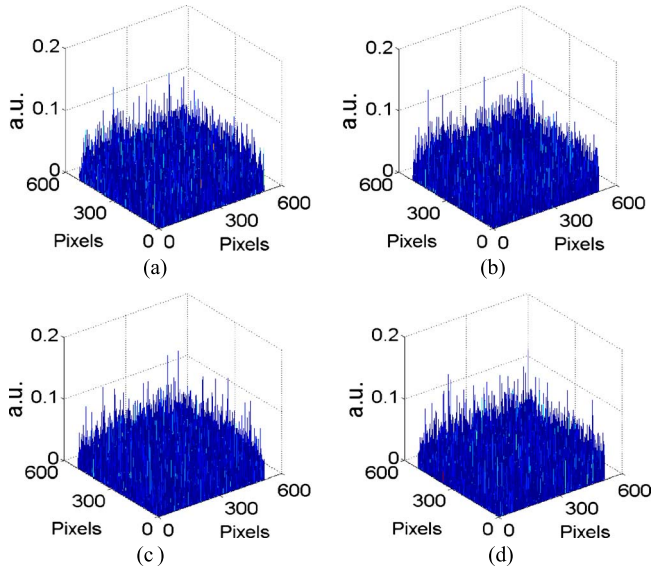

Fig. 6. (a)–(d) Generated nonlinear correlation distributions respectively corresponding to the decoded images in Fig. 5(a)–(d).

In practice, the encoded image should be transmitted to authorized receivers, and may be contaminated by some external influences, such as occlusion and noise. Here, system robustness against the contaminations is investigated. Fig. 7(a) shows the decoded image, when 25.0% pixels in the encoded image (i.e., binary diffraction intensity pattern) are occluded. The CC value for Fig. 7(a) is 4.37×10^{-2}. Fig. 7(c) shows the generated nonlinear correlation distribution corresponding to Fig. 7(a). Fig. 7(b) shows the decoded image, when the encoded image (i.e., binary diffraction intensity pattern) is contaminated by random noise [signal-to-noise ratio (SNR) of 1.0]. The random noise [35]–[37] is additive to the encoded image, and is generated by $(\{\text{Mean}[I(\mu, \nu)]\}/\text{SNR}) \times W$, where Mean denotes mean value and W is 2-D variable randomly distributed in a range of $[-1.5, 1.5]$. The CC value for Fig. 7(b) is 4.38×10^{-2}. Fig. 7(d) shows the generated nonlinear correlation distribution corresponding to Fig. 7(b). It is seen in Fig. 7(c) and (d) that the decoded images can still be correctly verified, and high robustness against contaminations is achieved in the proposed optical system.

Performance of the proposed method is further tested, when another input image (see the second one in inset of Fig. 1) is encoded based on the proposed optical system using the same parameters as those used for Fig. 4. Fig. 8(a) shows the decoded image, when all keys are correctly applied during the decoding. Due to the designed optical encoding strategy using a binary intensity pattern, it is also illustrated that information related to the second input image cannot be clearly observed from the decoded image. Fig. 8(b) shows the corresponding nonlinear

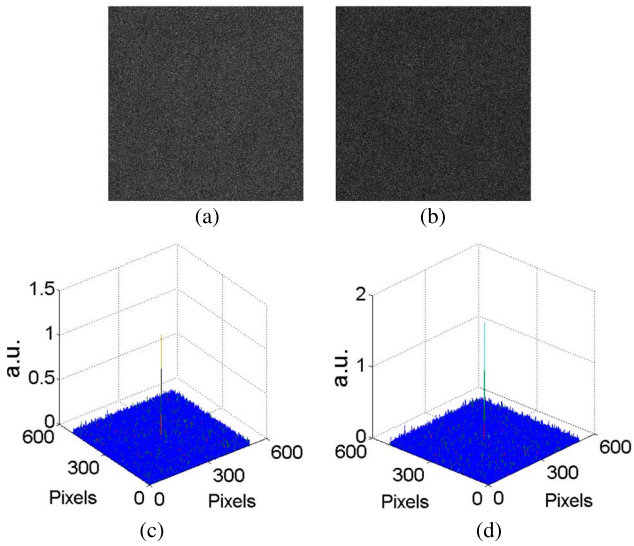

Fig. 7. System robustness against the contaminations. (a) Decoded image obtained when some pixels in the encoded image (i.e., binary diffraction intensity pattern) are occluded, (b) decoded image obtained when the encoded image (i.e., binary diffraction intensity pattern) is contaminated by random noise, and (c) and (d) the generated nonlinear correlation distributions, respectively, corresponding to (a) and (b).

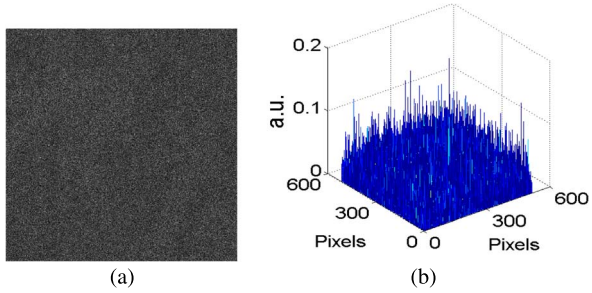

Fig. 8. Discrimination capability. (a) Decoded image obtained when all keys are correctly applied and (b) the corresponding nonlinear correlation map between that in (a) and the original input image (i.e., the first input image in inset of Fig. 1).

correlation map between that in Fig. 8(a) and the original input image (i.e., the first input image in inset of Fig. 1). As seen in Fig. 8(b), only noisy background is generated in the nonlinear correlation distribution, and the proposed method possesses high discrimination capability. The tests have been done using a series of different grayscale input images, and similar results as those in Fig. 8(a) and (b) can be obtained.

It has been illustrated that when a low-pass filter [32] is applied to process the amplitude part of complex-valued wavefront $\hat{O}^{(n)}(x, y)$ [obtained in (5)] at the first several iterations, the quality of decoded image can be improved. Here, it is demonstrated that use of the low-pass filter still cannot result in the visibility of decoded images in the proposed optical system, since only one binary diffraction intensity pattern is available in this study. Fig. 9(a) shows a relationship between the number of iterations and iterative errors (logarithm scale) at the first iteration stage (i.e., with low-pass filter during the first several iterations), and Fig. 9(b) shows a relationship between the number of iterations and iterative errors (logarithm scale) at the second iteration stage (i.e., without filter). Fig. 9(c) shows the decoded image when all keys are correctly applied. The CC value for Fig. 9(c) is 5.75×10^{-2}. It is seen in Fig. 9(c) that the decoded image cannot visually render the input information, which still satisfies the major objective of this study. Fig. 9(d)

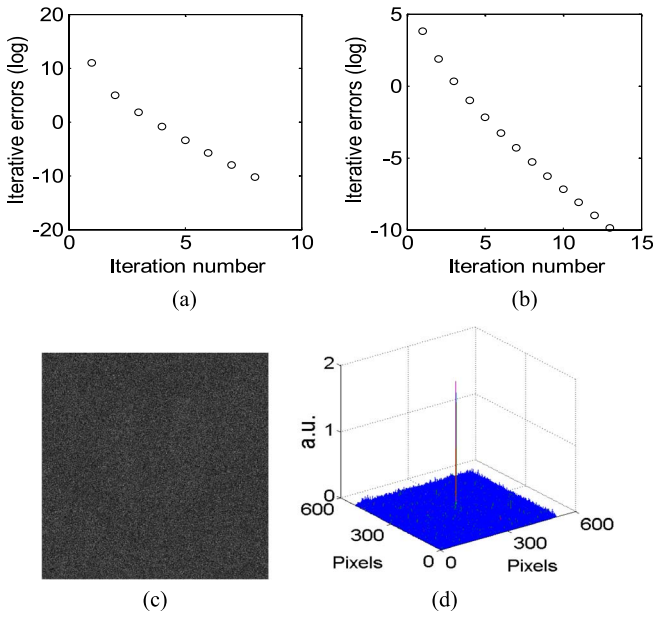

Fig. 9. (a) Relationship between the number of iterations and iterative errors (logarithm scale) at the first iteration stage (i.e., with a low-pass filter during the first several iterations), (b) relationship between the number of iterations and iterative errors (logarithm scale) at the second iteration stage (i.e., without low-pass filter), (c) the decoded image obtained when all keys are correctly applied, and (d) the generated nonlinear correlation distribution corresponding to (c).

shows the generated nonlinear correlation distribution corresponding to Fig. 9(c). Only one remarkable peak is also observed, and the decoded image is effectively verified.

4. Conclusion

A method has been proposed for optically verifying the decoded images in the DRPE system based on single-shot imaging without reference wave using binary intensity pattern, and it is the first to report the use of only one 1-bit intensity pattern in the DRPE system for secured verification via optical image correlation. During optical encoding, the encoded image with only two quantization levels is obtained by using single-shot imaging without reference wave based on DRPE infrastructure. The computational results demonstrate that decoded images obtained by iterative phase retrieval algorithm do not visually render the input information due to the designed optical encoding strategy using a binary intensity pattern, and optical verification can be further applied to effectively authenticate the decoded images.

References

[1] P. Refregier and B. Javidi, "Optical image encryption based on input plane and Fourier plane random encoding," *Opt. Lett.*, vol. 20, no. 7, pp. 767–769, Apr. 1995.
[2] B. Javidi, "Securing information with optical technologies," *Phys. Today*, vol. 50, no. 3, pp. 27–32, Mar. 1997.
[3] W. Chen, B. Javidi, and X. Chen, "Advances in optical security systems," *Adv. Opt. Photon.*, vol. 6, no. 2, pp. 120–155, Jun. 2014.
[4] E. Pérez-Cabré, H. C. Abril, M. S. Millán, and B. Javidi, "Photon-counting double-random-phase encoding for secure image verification and retrieval," *J. Opt.*, vol. 14, no. 9, Sep. 2012, Art. ID 094001.
[5] O. Matoba, T. Nomura, E. P. Cabré, M. S. Millán, and B. Javidi, "Optical techniques for information security," *Proc. IEEE*, vol. 97, no. 6, pp. 1128–1148, Jun. 2009.
[6] O. Matoba and B. Javidi, "Encrypted optical memory system using three-dimensional keys in the Fresnel domain," *Opt. Lett.*, vol. 24, no. 11, pp. 762–764, Jun. 1999.
[7] G. Situ and J. Zhang, "Double random-phase encoding in the Fresnel domain," *Opt. Lett.*, vol. 29, no. 14, pp. 1584–1586, Jul. 2004.

[8] G. Unnikrishnan, J. Joseph, and K. Singh, "Optical encryption by double-random phase encoding in the fractional Fourier domain," *Opt. Lett.*, vol. 25, no. 12, pp. 887–889, Jun. 2000.
[9] X. Wang and D. Zhao, "Amplitude-phase retrieval attack free cryptosystem based on direct attack to phase-truncated Fourier-transform-based encryption using a random amplitude mask," *Opt. Lett.*, vol. 38, no. 18, pp. 3684–3686, Sep. 2013.
[10] L. Sui, K. Duan, J. Liang, and X. Hei, "Asymmetric double-image encryption based on cascaded discrete fractional random transform and logistic maps," *Opt. Exp.*, vol. 22, no. 9, pp. 10 605–10 621, May 2014.
[11] X. Wang, W. Chen, S. Mei, and X. Chen, "Optically secured information retrieval using two authenticated phase-only masks," *Sci. Rep.*, vol. 5, Oct. 2015, Art. ID 15668.
[12] W. Chen, X. Chen, and C. J. R. Sheppard, "Optical image encryption based on diffractive imaging," *Opt. Lett.*, vol. 35, no. 22, pp. 3817–3819, Nov. 2010.
[13] X. Peng, H. Wei, and P. Zhang, "Asymmetric cryptography based on wavefront sensing," *Opt. Lett.*, vol. 31, no. 24, pp. 3579–3581, Dec. 2006.
[14] W. Qin and X. Peng, "Asymmetric cryptosystem based on phase-truncated Fourier transforms," *Opt. Lett.*, vol. 35, no. 2, pp. 118–120, Jan. 2010.
[15] W. Chen and X. Chen, "Ghost imaging for three-dimensional optical security," *Appl. Phys. Lett.*, vol. 103, no. 22, Nov. 2013, Art. ID 221106.
[16] W. Chen, G. Situ, and X. Chen, "High-flexibility optical encryption via aperture movement," *Opt. Exp.*, vol. 21, no. 21, pp. 24680–24691, Oct. 2013.
[17] X. F. Meng *et al.,* "Hierarchical image encryption based on cascaded iterative phase retrieval algorithm in the Fresnel domain," *J. Opt. A, Pure Appl. Opt.*, vol. 9, no. 11, pp. 1070–1075, Oct. 2007.
[18] Z. Liu, Q. Guo, L. Xu, M. A. Ahmad, and S. Liu, "Double image encryption by using iterative random binary encoding in gyrator domains," *Opt. Exp.*, vol. 18, no. 11, pp. 12 033–12 043, May 2010.
[19] J. Liu, X. Xu, Q. Wu, J. T. Sheridan, and G. Situ, "Information encryption in phase space," *Opt. Lett.*, vol. 40, no. 6, pp. 859–862, Mar. 2015.
[20] A. Carnicer, M. M. Usategui, S. Arcos, and I. Juvells, "Vulnerability to chosen-cyphertext attacks of optical encryption schemes based on double random phase keys," *Opt. Lett.*, vol. 30, no. 13, pp. 1644–1646, Jul. 2005.
[21] B. Hennelly and J. T. Sheridan, "Optical image encryption by random shifting in fractional Fourier domains," *Opt. Lett.*, vol. 28, no. 4, pp. 269–271, Feb. 2003.
[22] M. He, Q. Tan, L. Cao, Q. He, and G. Jin, "Security enhanced optical encryption system by random phase key and permutation key," *Opt. Exp.*, vol. 17, no. 25, pp. 22462–22473, Dec. 2009.
[23] Y. Frauel, A. Castro, T. J. Naughton, and B. Javidi, "Resistance of the double random phase encryption against various attacks," *Opt. Exp.*, vol. 15, no. 16, pp. 10253–10265, Aug. 2007.
[24] P. Kumar, A. Kumar, J. Joseph, and K. Singh, "Impulse attack free double-random-phase encryption scheme with randomized lens-phase functions," *Opt. Lett.*, vol. 34, no. 3, pp. 331–333, Feb. 2009.
[25] E. Pérez-Cabré, M. Cho, and B. Javidi, "Information authentication using photon-counting double-random-phase encrypted images," *Opt. Lett.*, vol. 36, no. 1, pp. 22–24, Jan. 2011.
[26] D. Maluenda, A. Carnicer, R. Martínez-Herrero, I. Juvells, and B. Javidi, "Optical encryption using photon-counting polarimetric imaging," *Opt. Exp.*, vol. 23, no. 2, pp. 655–666, Jan. 2015.
[27] W. Chen, X. Chen, A. Stern, and B. Javidi, "Phase-modulated optical system with sparse representation for information encoding and authentication," *IEEE Photon. J.*, vol. 5, no. 2, Apr. 2013, Art. ID 6900113.
[28] J. W. Goodman, *Introduction to Fourier Optics*, 2nd ed. New York, NY, USA: McGraw-Hill, 1996.
[29] F. Yang, Y. M. Lu, L. Sbaiz, and M. Vetterli, "Bits from photons: Oversampled image acquisition using binary Poisson statistics," *IEEE Trans. Image Process.*, vol. 21, no. 4, pp. 1421–1436, Apr. 2012.
[30] C. Shoushun and A. Bermak, "Arbitrated time-to-first spike CMOS image sensor with on-chip histogram equalization," *IEEE Trans. Very Large Scale Integr. (VLSI) Syst.*, vol. 15, no. 3, pp. 346–357, Mar. 2007.
[31] R. W. Gerchberg and W. O. Saxton, "A practical algorithm for the determination of phase from image and diffraction plane pictures," *Optik*, vol. 35, no. 2, pp. 237–246, Nov. 1972.
[32] Y. Qin, Q. Gong, and Z. Wang, "Simplified optical image encryption approach using single diffraction pattern in diffractive-imaging-based scheme," *Opt. Exp.*, vol. 22, no. 18, pp. 21790–21799, Sep. 2014.
[33] W. Chen, "Multiple-wavelength double random phase encoding with CCD-plane sparse-phase multiplexing for optical information verification," *Appl. Opt.*, vol. 54, no. 36, pp. 10711–10716, Dec. 2015.
[34] W. Chen and X. Chen, "Grayscale object authentication based on ghost imaging using binary signals," *Eur. Phys. Lett.*, vol. 110, no. 4, May 2015, Art. ID 44002.
[35] W. Chen and X. Chen, "Focal-plane detection and object reconstruction in the noninterferometric phase imaging," *J. Opt. Soc. Amer. A, Opt. Image Sci.*, vol. 29, no. 4, pp. 585–592, Apr. 2012.
[36] C. Wu, T. W. Ng, and A. Neild, "Phase and amplitude retrieval of objects embedded in a sinusoidal background from its diffraction pattern," *Appl. Opt.*, vol. 49, no. 10, pp. 1831–1837, Apr. 2010.
[37] W. Chen and X. Chen, "Quantitative phase retrieval of complex-valued specimens based on noninterferometric imaging," *Appl. Opt.*, vol. 50, no. 14, pp. 2008–2015, May 2011.